Chapter 5
Detection of Small and Noisy Signals in Sensor Interfacing: The Analog Lock-in Amplifier

In this chapter, firstly the main methods for the signal recovery from noise will be introduced and discussed. Then, the lock-in technique, for the detection of sensor signals embedded into noise, will be described in detail. In this sense, an analog lock-in amplifier (to be used in sensor interfaces) as a complete integrated circuit, designed at transistor level in a standard *CMOS* technology (AMS 0.35 μm), will be presented, together with some experimental results on gas sensors. This integrated solution improves sensitivity and resolution of the complete gas measurement system. Finally, we also propose the block scheme and operation of a high-precision high-accuracy fully-automatic integrable analog lock-in amplifier, also employed for the detection of small quantities of gases.

5.1 Signal Recovery Techniques Overview: The SNR Enhancement

Recovering a signal from noise allows to improve the Signal to Noise ratio (*SNR*). This can be done by reducing the noise accompanying a signal, through the following two basic techniques:

- bandwidth reduction, where the noise is decreased by reducing the system noise bandwidth (B_n). This approach works well if the frequency spectra of the noise and signal do not overlap significantly, so that reducing the noise bandwidth does not affect the signal. For a random white noise, the output noise is proportional to $\sqrt{B_n}$ (for a non-white noise, other relationships must be considered);
- averaging or integrating techniques, where consecutive samples of the signal are synchronized and added together. The signal grows as the number (n) of added samples, while, considering random white noise, the noise grows as $\sqrt{n}$. This is true if the signal characteristics are stationary for the duration of the extraction process.

A. De Marcellis and G. Ferri, *Analog Circuits and Systems for Voltage-Mode and Current-Mode Sensor Interfacing Applications*, Analog Circuits and Signal Processing,
DOI 10.1007/978-90-481-9828-3_5, © Springer Science+Business Media B.V. 2011

The bandwidth reduction technique is best looked at from a frequency-domain point of view; on the contrary, signal averaging and correlation techniques lend themselves to time-domain analysis. Sometimes it is useful to combine both these techniques. In many applications, there is a significant overlap between the signal and noise spectra and improving a *SNR* must be done at the expense of the response time or measurement time (T); for random white noise, the output *SNR* is proportional to $\sqrt{T}$.

For further simplicity, it is assumed that all noise processes are stationary and that both signal and noise are ergodic, analog variables; in the following, digital signals or discrete-time (sampled) signals will not be taken into account, except where such signals are involved in the analog enhancement techniques. They are essential in modern application methods but it is the basic idea that drives the digital methods. Therefore, only signal recovery techniques will be considered. Further processing, such as least-squares polynomial smoothing of a waveform or Fourier transformation to obtain a frequency spectrum, are not considered here.

Let us present now a classification of the *SNR* enhancement techniques to be applied in sensor interfacing, especially when the *SNR* is < 1 or $\ll 1$. Since small size and low energy sensors often provide extremely low levels of output signals to be measured under the presence of a noisy environment, a suitable signal processing operation is required to obtain relevant information. Moreover, it is even possible that the power of the superimposed noise and interferences is larger than the power of the signal of interest. Generally, in such circumstances, a linear filtering operation is not sufficient to extract the signal information, so special techniques for enhancing the *SNR* have to be adopted [1–12].

More in detail, starting from the main basic classification previously described, it is possible to considerate the following three main electronic (analog and/or digital) systems [1]:

- waveform averagers
  - box car integrators
  - signal averagers
- correlation function calculators
  - autocorrelators
  - crosscorrelators
- lock-in amplifiers (analog or digital)

It is important to highlight the relationship between the input signal (to be recovered) and the reference one (if required). In particular, concerning waveform averages, which utilize techniques for signal averaging, the following conditions have to be satisfied: the input signal has to be repetitive, even if it is not periodic; the input signal has to be either preceded by a trigger pulse or able to provide a pulse at a certain time, before of the sampling time; the input signal and trigger pulse have to be synchronized; the input signal has to be as much as possible without "jitters" which can cause errors in some cases. As regards autocorrelators and

crosscorrelators, the input signal to be recovered does not require any synchronized trigger pulse. In particular, when the same signal is compared to phase shifted copies of itself, the procedure is known as autocorrelation, while when two independent signals are compared the procedure is known as crosscorrelation. On the contrary, lock-in amplifiers require that the input signal is periodic and has a fixed and well-known frequency so a reference signal having the same frequency and a suitable phase condition has to be provided.

More in detail, a waveform averager samples the applied signal at a regular sampling rate and stores the resulting waveform. It can repeat this process so that a periodic input signal can be monitored in exactly the same way on each new cycle. Each record is added to the sum of the previous records so that a continuous summation process takes place. Any asynchronous event (i.e., noise) will be reduced in amplitude in relation to the amplitude of the synchronous events (i.e., signal) and hence the summed record represents the original signal waveform recovered from the noise. In the case of Gaussian noise, the improvement in *SNR* gained from this process is approximately equal to the square root of the number of summed cycles. Hence, for example, averaging 100 records of an identical event will improve the *SNR* by ten times.

As mentioned above, the main significant types of averagers, which can be utilized when the input signal has harmonic components in a wide frequency range, are the box-car integrators and the signal averagers.

The box-car integrator (which can be stationary, scanning mode or multichannel) typically utilizes analog electronics, supported by digital control, to monitor one discrete point in time on a repetitive signal. It is based on the sampling of the input signal, at a fixed time, in a defined time interval (the so-called "gate time"). The sampling is always controlled by a suitable trigger pulse depending on the same input signal. In particular, it builds up an average of that point over many cycles before recording it as a value. It may then move on to a different (later) point and repeat the process, averaging for the same number of cycles as for the first point, before recording a second value. In this way it can "step" across a waveform, monitoring it at discrete points to build up a complete averaged representation of the input signal.

The signal averager uses digital techniques to record all of the waveforms on each cycle. This makes it much more time efficient than box-car systems. Nonetheless the time taken to do the summation limits the maximum data throughput unless a dedicated hardware averager is included.

Therefore, box-car systems are particularly well suited to average a single point in time repetitively. As an example, the amplitude of one peak of a spectrum, derived from a repetitively swept monochromator, could be averaged easily and recorded as a function of time using a box-car system. This technology can also give a good time resolution, lower than 1 ns. Signal averagers can provide maximum time resolutions of a similar level, but are better suited to waveform recovery and to monitoring short lived phenomena due to their better time efficiency.

The correlation techniques (i.e., correlation function calculators) for the *SNR* improvement regard the existing relationship between either a signal to be revealed

and an its delayed copy (autocorrelation) or two different signals (crosscorrelation). A function which is related to the correlation function, but arithmetically less complex, is the average magnitude difference function.

In particular, the autocorrelation function allows to extract an information (i.e., the amplitude of the signal), buried into noise, but the same kind of operation is not suitable to reveal also the information related to the signal phase. Moreover, this operation can provide, as a result, also a function which is completely different from that utilized as input data in the autocorrelation operation, depending on the kind of input waveform. It is important to consider that, for example, the autocorrelation of the "white" noise, having a wide bandwidth, provide as a result a correlation function which tends to zero with a decay time depending on its bandwidth; moreover, since this kind of noise is completely random and has not any temporal correlation, its resulting autocorrelation is a "delta" function. Therefore, when a sinusoidal signal is buried into noise (also with a reduced bandwidth), the autocorrelation function provides two contributes: one related to the noise, which decays to zero, and the other, associated to the sinusoidal signal, which will be extracted after a suitable time delay, being still a sinusoidal waveform from which it is possible to extract the desired information related to the amplitude value of the AC component (i.e., the peak value of the input sinusoidal signal).

The crosscorrelation function is similar to the autocorrelation one, but in this case the delayed signal, to be multiplied with the input signal, comes from another source. As a consequence, this technique provides, as a correlation result, the frequency components which are common to both the two input signals. The advantage provided by the crosscorrelation is in the very strong rejection to noise and disturbs. In fact, when there is no correlation between the input signal and the noise, the resulting signal coming from crosscorrelation, for a suitable long measuring time, tends to zero.

Autocorrelation is a method which is frequently used for the extraction of a fundamental frequency (f_0): if a copy of the signal is shifted in phase, the distance between correlation peaks is taken to be the fundamental period of the signal (directly related to f_0). The method may be combined either with the simple smoothing operations of peak and centre clipping or with other low-pass filter operations. On the contrary, crosscorrelation is the method which basically underlies implementations of the Fourier transformation: signals of varying frequency and phase are correlated with the input signal and the degree of correlation in terms of frequency and phase represents the frequency and phase spectrums of the input signal.

Finally, lock-in amplifiers (analog or digital) are extremely powerful signal recovery instruments if the signal is, or can be made to be, an amplitude-modulated AC waveform, where the envelope of the modulation is the required output. In fact, a lock-in amplifier, based on a phase sensitive detector, provides a DC output voltage signal which is proportional to the root mean square value of the AC input noisy signal (typically, slowly time variable). Generally, long time constants can increase the accuracy of the measurement system by averaging out AC noise, but if the meter itself experiences DC drifts during that time, the measurements cannot be valid and,

in addition, a very long time constant occur. On the contrary, the lock-in technique provides for rejecting both AC and DC noise sources before the signal is measured. Typically, in lock-in amplifiers the measured signal can be averaged to much shorter time constants, allowing faster and more accurate results [2–12].

More in detail, also referring to sensor microsystems, the application of lock-in principle to extract, in a synchronous way, signal from noise is possible under the condition that the noisy signal (e.g., coming from the sensor) has a fixed and well-known frequency [13–18]. In particular, the lock-in technique, operating with a single reference frequency, can be utilized in electronic interfaces and optical sensor applications for recovering signal from noise or, in alternative, to operate very high-resolution measures of "clean" or "noisy" signals with different amplitudes and frequencies.

In the next Paragraphs, analog lock-in amplifiers will be described and their application to sensor interface to enhance system sensitivity and resolution is proved.

5.2 The Lock-in Amplifier

The lock-in amplifier measures the magnitude of a signal in a very narrow frequency bandwidth, while rejects all the components of the signal that are outside it. The lock-in technique has revealed to be better than a simple filtering operation, thanks to its superior performance. In fact, because of the automatic tracking, lock-in amplifiers can give effective quality factor Q values (a measure of filter selectivity) over 100,000, whereas a normal band-pass filter becomes difficult to use with a Q greater than 50.

Its main active block is the Phase-Sensitive Detector (*PSD*): it is a "special waveform rectifier", performing an AC-to-DC conversion, which increases only the useful signal while reduces the noise effect overlapped to the same signal. In order to properly work, the *PSD* has to be excited by a reference signal having the same frequency of the input noisy signal and a suitable phase delay. The use of this "locked" reference (from which the technique takes its name) assures the capability of the system to pursue the input noisy signal increasing its *SNR*. In fact, the system reduces the noise bandwidth through a synchronous operation which needs the knowledge of the useful signal frequency, giving a *SNR* improvement equal to the ratio between the *SNR* at the lock-in output and that at its input.

In order to recover a signal from noise, the lock-in amplifier must be provided with a relatively clean reference signal of the same frequency as the signal to be measured. Therefore, lock-in amplifiers can use a Phase-Locked-Loop (*PLL*) to generate the reference signal, otherwise an external reference signal must be provided. In particular, in the lock-in system, the *PLL* locks the internal reference oscillator to the external signal, resulting in a reference waveform with a proper phase shift. Since the *PLL* actively tracks the external signal, changes in the external reference frequency do not affect the measurement. Moreover, if the input noisy signal to be measured is of DC kind, it must be opportunely modulated by an AC

waveform either electrically (e.g., as in exciting a strain gauge with an AC voltage) or mechanically (e.g., as in passing a light beam through an optical chopper). The signal and its modulation frequency (the reference signal) can be then easily fed to a lock-in amplifier.

Lock-in amplifiers can be of analog or digital kind. Those which use an analog signal processing channel are invariably known as analog instruments, even if sometimes they include digital output filters. The term "digital lock-in amplifier" usually refers to units which utilize a *DSP* demodulator. In fact, although there is a commercially available instrument described as a high-frequency *DSP* lock-in amplifier, it is an analog unit used as a "down converter" followed by a low frequency *DSP* final detector stage. *DSP* instruments generally give better performance than their analog counterparts and have inevitably become the first choice for the user. However, it is worth remembering that there are still some applications for which the analog instruments will offer different advantages (e.g., higher operating frequencies, since *DSP* units are currently restricted to operation at about few MHz or below, whereas analog units can operate to many MHz). Among these, we mention the use of lock-in amplifiers as first analog front-ends in sensor applications when the information coming from sensor systems can be very small and buried into noise. This allows to detect very small quantities of measurands as, for an example, few ppm (or ppb) of target gases.

In the following, the basic operation of an analog lock-in amplifier will be described more in detail so to better understand how this system works and how the choices made in their design influence its performances.

In Fig. 5.1 a possible block scheme of an analog lock-in amplifier implementation is shown. It is possible to highlight two different channels: the input and the reference signal channels. The first active block, which processes the input noisy signal, is a Low Noise Amplifier (*LNA*). It provides a high DC gain, adding noise as small as possible, to the input signal. Since the spectrum of the signal of interest

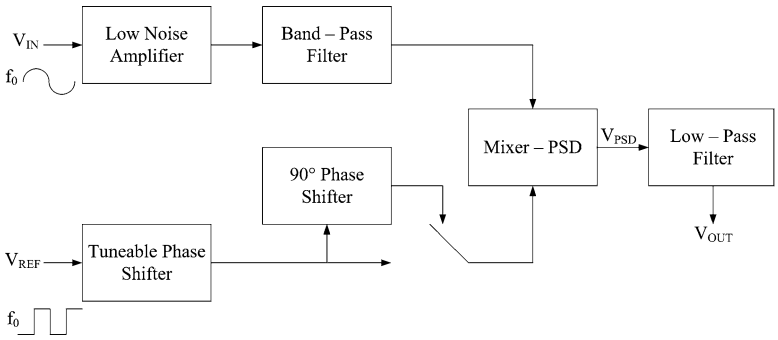

Fig. 5.1 Basic block scheme of an analog lock-in amplifier architecture. *Upper path*: input signal channel. *Lower path*: reference signal channel (V_{IN} = AC input signal, V_{REF} = AC reference signal, V_{PSD} = mixer output signal, V_{OUT} = DC output signal)

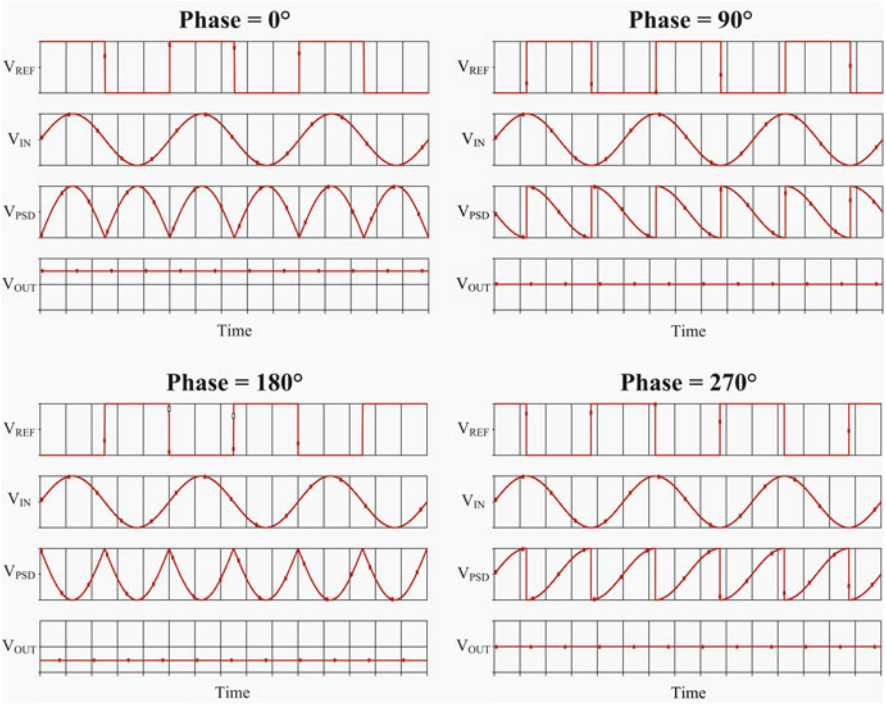

Fig. 5.2 Main signals in the lock-in amplifier for various phase differences between the input signal of interest and the reference signal

is zero for all frequencies but the signal operating frequency f_0, a suitable band-pass filter, whose center frequency must be exactly f_0, can increases the *SNR*. In the reference signal channel, different phase shifters must be used in order to both null and put "in quadrature" the phase difference between the reference signal and input signal (e.g., coming from a sensor). In particular, the relative phase of reference signal can be easily synchronized with the input signal through two active blocks: a tunable phase shifter and a 90° fixed phase shifter. In this way, the next block, a mixer or *PSD*, generates a periodic signal, whose DC component is proportional to the amplitude of AC input signal and depends from mentioned phase difference, as shown in Fig. 5.2: if the phase difference between the reference signal and the signal of interest is 0° or 180°, the output signal has a non-zero DC component which is proportional to the amplitude of the input signal. The signal generated by the mixer may easily be extracted by means of a suitable low-pass filter, which represents the final block of the complete system. In order to pull out exactly the DC component, from the periodic signal generated by the mixer, a suitable choice of the low-pass filter cut-off frequency (possibly the lowest) must be done.

Lock-in amplifiers can be seen as very narrow filters with a central frequency f_0 and a quality factor Q which, neglecting the band-pass filtering, can be expressed as following:

$$Q = \frac{f_0}{\Delta f} \tag{5.1}$$

where Δf is the band-width of the low-pass filter. Obviously, the smaller the bandwidth of the low pass filter is, the higher both the Q and the rejection of the disturbances are; on the other hand, the complete system may not be faster than the low pass filter itself, so a trade-off exists between the Q value (related to the disturbance rejection) and the speed (i.e., time response) of the lock-in amplifier (in other words, better results require long measurement times).

In order to express the lock-in amplifier *SNR* improvement quantitatively, we have that the *SNR* at the output of the lock-in amplifier is given by the *SNR* at the input multiplied by the square root of the ratio between the equivalent noise bandwidth and the bandwidth of the low pass filter, as reported in the following expression:

$$SNR_{OUT} = SNR_{IN}\sqrt{\frac{B_{EQ\_NOISE}}{B_{LPF}}} \tag{5.2}$$

Therefore, as an example, if the equivalent noise bandwidth is 10^4 Hz and the bandwidth of the low pass filter is 10^{-2} Hz, the *SNR* improvement is 10^3. On the other hand, the advantage of the lock-in amplifier, with respect to a conventional filter, is in the fact that the system bandwidth (i.e., the bandwidth of the low pass filter) can be imposed orders of magnitude lower than that related to a conventional filtering device.

Finally, it is important to highlight that the basic architecture reported in Fig. 5.1 can be conveniently integrated into a single chip, after a suitable design of the single blocks at transistor level, as demonstrated in the next Paragraph; therefore, the lock-in amplifier is also suitable for portable sensor applications [1–12].

5.3 An Integrated LV LP Analog Lock-in Amplifier for Low Concentration Detection of Gas

Commercial lock-in amplifiers typically show large dimensions, high costs and are not suitable for portable applications. In the literature, both digital and analog lock-in amplifiers for sensor applications have been presented (e.g., in [13–18]).

Recently, a low-cost integrated analog lock-in amplifier, powered by a low dual supply voltage (± 1 V) and showing low power consumption (3 mW), has been proposed. It has been also used as a part of the first sensor analog front-end and has been introduced in a sensor system with the aim to detect very low quantities of dangerous gases [19, 20].

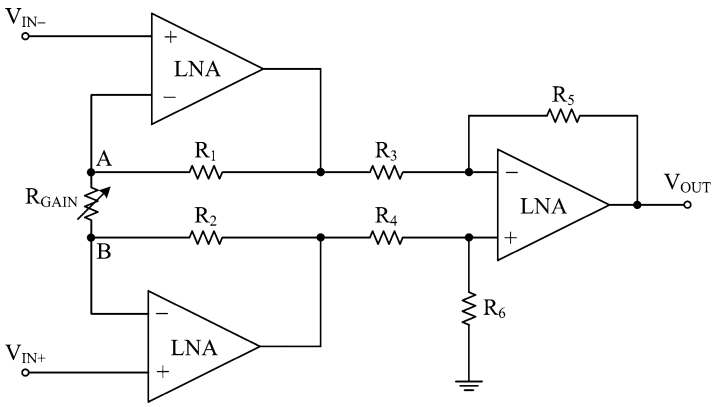

Fig. 5.3 Traditional differential input instrumentation voltage amplifier implemented by LNA

The proposed lock-in amplifier has been designed, at transistor level in a standard *CMOS* technology (AMS 0.35 μm), in order to work at a low fixed operating frequency $f_0 = 77$ Hz. This value has been chosen so to reduce, as much as possible, any kind of interference with the net supply oscillation frequency (50 Hz) and its harmonics. Moreover, this frequency is also compatible with typical characteristics of the resistive gas sensor. The presented lock-in system, totally formed by analog blocks, has been integrated in a reduced silicon area (about 5 mm^2) and is able to reveal very small signals, also thanks to a particular design of its internal blocks and of the first amplifier stage showing very low noise characteristics. In particular, the latter has been designed in the configuration of a traditional *VM OA*-based instrumentation amplifier, as reported in Fig. 5.3. In order to achieve good noise and common mode rejection performances, a *LNA*, to be utilized in the three active blocks, has been designed at transistor level, according to the internal topology shown in Fig. 5.4. Since that, in the utilized technology, the *pMOS* transistors provide a noise factor K_f lower than *nMOS* transistors, *LNA* input stage has been based on a double *pMOS* differential pair (M_4–M_7), where each transistor has $W = 800\,\mu$ and $L = 20\,\mu$ sizes, so to provide a reduced input equivalent noise (about 22 nV/$\sqrt{}$Hz at 77 Hz reference frequency). The output stage, formed by M_{10} and M_{11}, is a class-AB Push-Pull inverter topology where frequency compensation has been obtained through the capacitance C_1, set to 1.5 pF. The complete AC differential amplifier provides a very high DC tuneable gain A (from 10 to 110 dB) and a very small input equivalent noise level. In particular, its DC gain can be simply set through the external variable resistance R_{GAIN}, as shown in Fig. 5.3, so the total equivalent input noise is about 34 nV/$\sqrt{}$ Hz at 77 Hz, for a 110 dB DC gain (obtained with $R_{GAIN} = 1\,\Omega$). Then, a band-pass filter has been implemented through the block scheme reported in Fig. 5.5. It uses only a single active component having the required specific central frequency, showing unitary voltage gain at central frequency and a quality factor Q of about 2. This not high value of Q has been chosen to avoid errors due to the variation of the central frequency owed

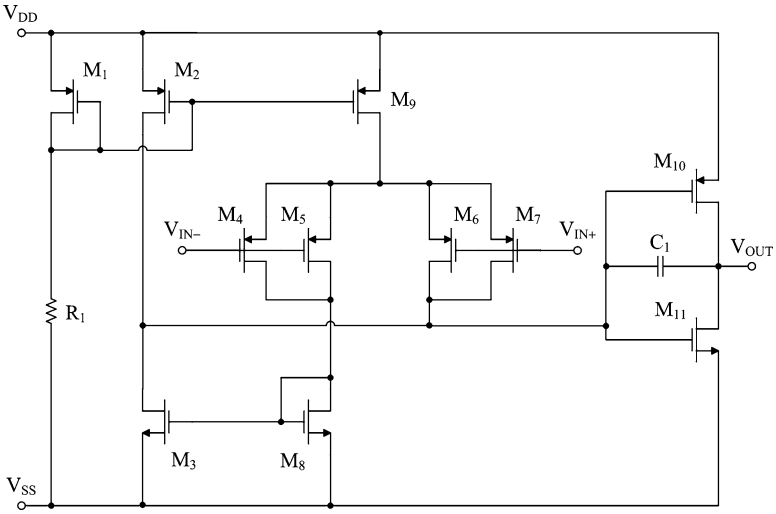

Fig. 5.4 Internal topology, at transistor level, of the implemented LNA

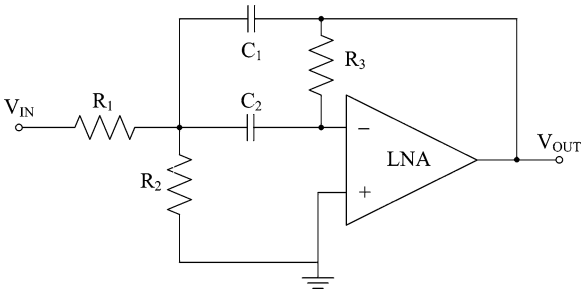

Fig. 5.5 Block scheme of the implemented active Bband-Ppass filter

to the non-idealities (e.g., aging, mismatch, temperature drift, operating condition, technological spread, etc.) of the employed passive and active components.

The mixer block is a wave rectifier that performs the multiplication between the amplified input signal and the reference signal having, as mentioned before, the same frequency f_0, but a different phase. It generates a proper periodic signal $V_{OUT,MIX}$, whose DC component is proportional to the amplitude of AC input signal V_{IN} and depends on this phase difference (φ), according to the following expression:

$$V_{OUT,MIX} = \frac{2}{\pi} k V_{IN} [\cos\varphi - \cos(2\omega_0 t + \varphi)] \tag{5.3}$$

being k the system total amplification (which takes into account also A).

Fig. 5.6 shows the block scheme of the implemented mixer, which utilizes the same *LNA* as main active block, together with two matched resistances R and two analog switches (S_1, S_2). The latter are controlled by the square wave reference

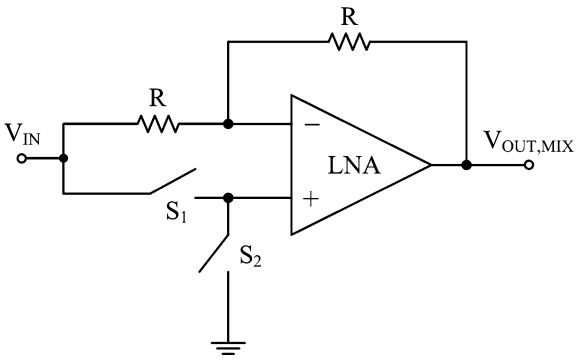

Fig. 5.6 Block scheme of the mixer or *PSD*

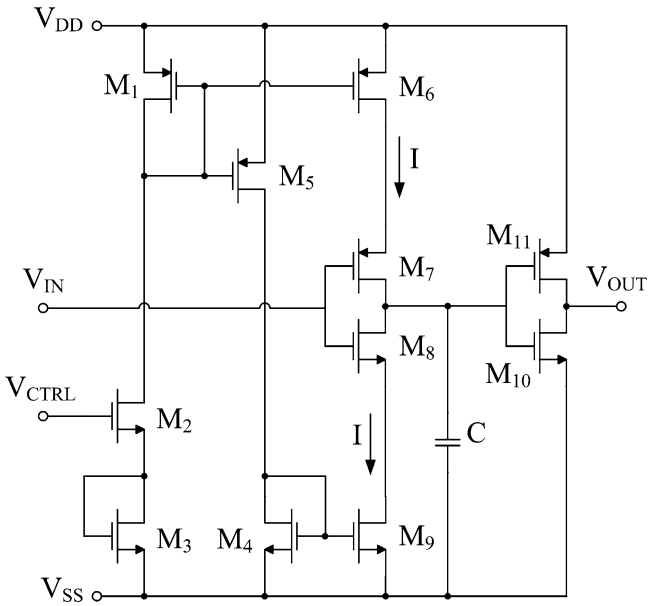

Fig. 5.7 Schematic circuit of the tunable phase shifter

signal which, through a *NOT* gate, is also inverted so to have two control lines in non overlapping phase-opposition. In this way, the switches are properly controlled since, referring to Fig. 5.6, when S_1 is open, S_2 is closed and vice versa. The gain of the mixer is ideally $+1$ or -1, depending on the relative phase between input and reference signals.

In order both to null and put in-quadrature the phase difference between the reference signal and that coming from the sensor (mixer input signals), a tuneable phase shifter and a 90° (fixed) phase shifter have been implemented, so to easily synchronize the two mixer inputs. Both of these blocks have been designed utilizing traditional internal circuit topologies, based on the cascade of two Push-Pull stages and the capacitance charge–discharge effect. Fig. 5.7 shows the schematic circuit, at

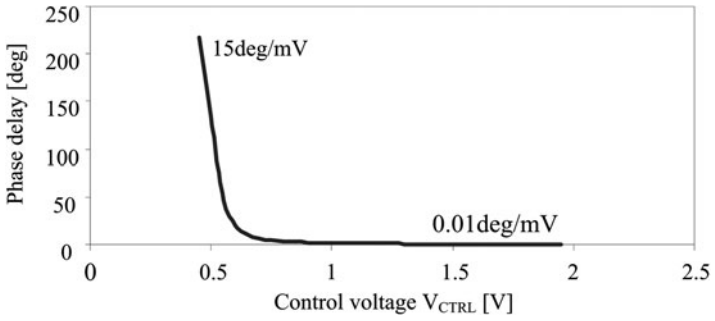

Fig. 5.8 The tuneable phase shifter: relationship between the phase delay, expressed in degree, and the applied external control voltage V_{CTRL}, showing two different sensitivity ranges

transistor level, of the designed tuneable phase shifter. In this scheme, C is charged through M_6 and M_7 and discharged through M_8 and M_9, with a constant current I. This circuit generates a time delay, thus a phase shifting, proportional to the capacitance value, according to the following expression:

$$T_{DELAY} = \frac{V_{DD} - V_{SS}}{2} \cdot \frac{C}{I} \tag{5.4}$$

being I the current shown in Fig. 5.7, whose value is determined by an external control voltage, V_{CTRL}. In order to perform a phase tuning in a large degree range, a cascade of four independent tuneable phase shifters has been implemented. In particular, the phase tuning can be easily performed, firstly, by activating the tuneable phase shifters through voltage controlled *CMOS* switches, and, then, by varying the single external control voltage V_{CTRL} (see always Fig. 5.7), so to tune the previously selected phase shifters. In this manner, it is possible both to properly regulate the current I which flows into the capacitances and to adjust the relative phase between input and reference signals.

Fig. 5.8 shows the relationship between the achieved phase delay, expressed in degree, and the applied external control voltage V_{CTRL}, highlighting two different sensitivity ranges. The 90°-phase shifter has been designed starting from the schematic circuit shown in Fig. 5.7 and adding two further Push-Pull stages and another capacitance. Through other suitable voltage controlled *CMOS* switches, it is possible to activate this shifter, so to provide exactly the required 90°.

The final block of the proposed complete architecture, which follows the mixer, is a low-pass filter that reduces the noise contribution through a DC extraction. The filter output is a DC voltage whose level is proportional to the amplitude of the input signal. An active low-pass filter based on a Transconductance active block (*Gm*), which, together with a capacitance C_{Gm}, allows to obtain a *Gm-C* integrator cell, has been designed, as it shown in Fig. 5.9. A fourth order low-pass filter has been simply obtained by cascading four *Gm-C* cells, having chosen all the capacitances C_{Gm} equal to 100 pF. Fig. 5.10 shows the internal topology of the

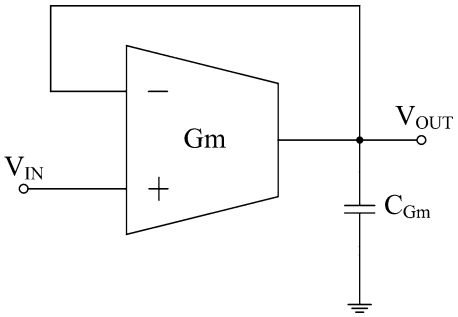

Fig. 5.9 Block scheme of a single Gm-C cell implementing an active low-pass filter

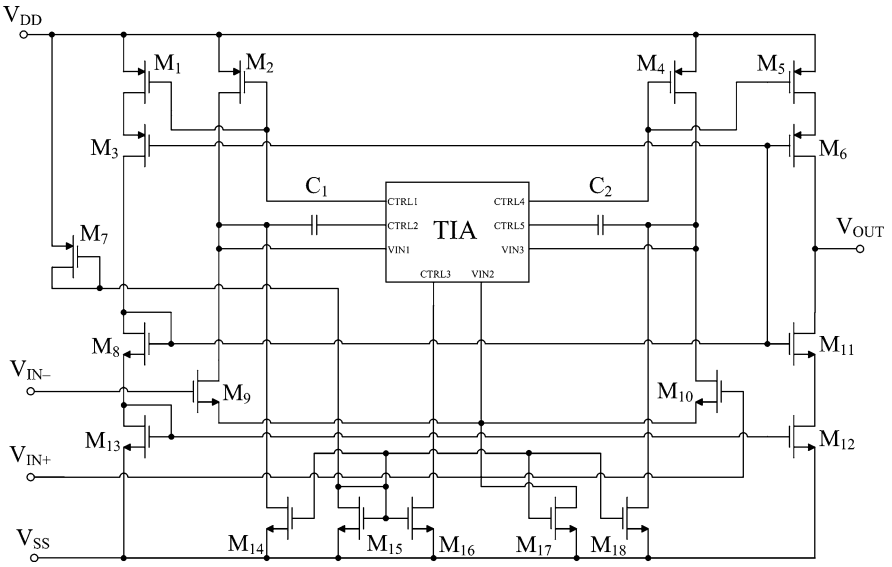

Fig. 5.10 Internal topology of the Gm block

designed Transconductance blocks, implemented through a Three Input Amplifier (*TIA*) [21], which allows to achieve a very low cut-off frequency, of about 1 mHz. Fig. 5.11 shows the circuit schematic at transistor level, of the designed *TIA*.

Fig. 5.12 shows the photo of the integrated lock-in, highlighted, on the left, by the arrow. A prototype *PCB* has been fabricated and utilized for the complete system on-chip testing. Fig. 5.13a, b depict the measured signals generated by the mixer, when a clean input signal and the reference signal are "in-quadrature" and "in-phase", respectively. Fig. 5.14a, b show the generated input noisy signal and the corresponding time response of the DC voltage signal at the system output. In particular, we detect a null response, related to "in-quadrature" mixer inputs, and a non-zero DC signal, with its transient response, achieved through the activation of the 90°-phase shifter ("in-phase" mixer inputs).

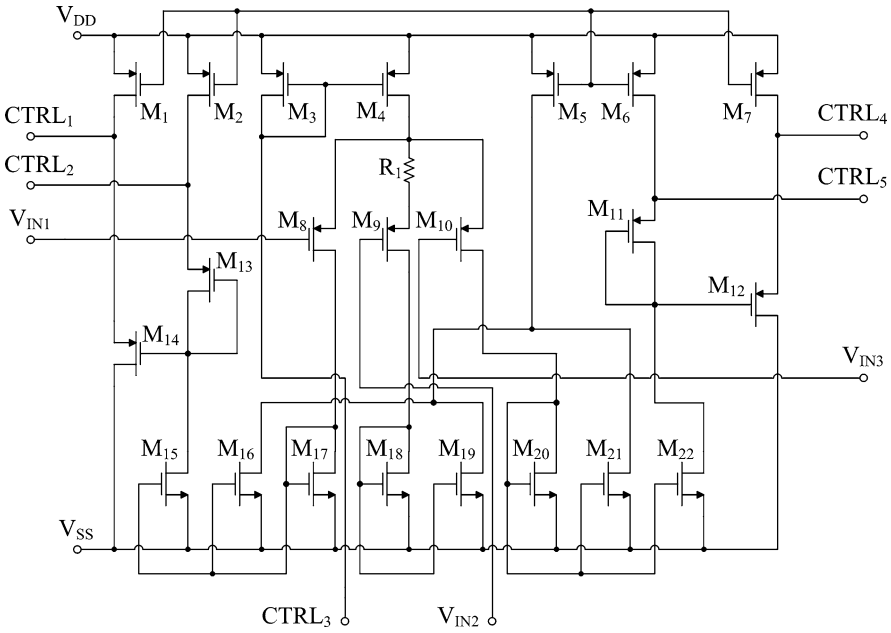

Fig. 5.11 The designed TIA circuit schematic at transistor level

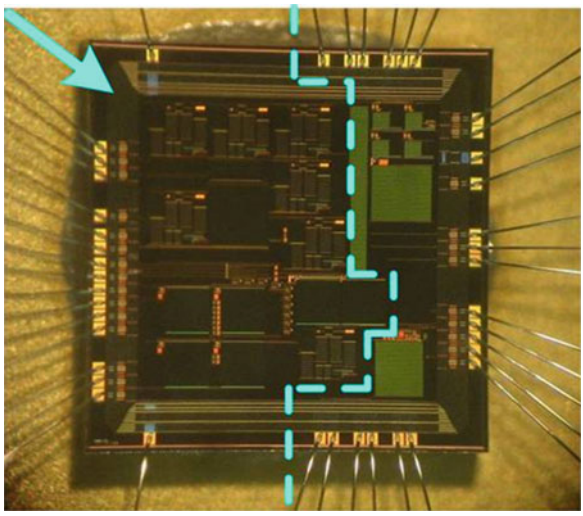

Fig. 5.12 Photo of fabricated chip: the designed lock-in is in the *left part*, delimited by the *dashed line*

This analog lock-in system is able to recover with success very small noisy signals (down to about 500 nV, with $SNR < 1$) without performance degradation. In particular, measurement results are reported in Fig. 5.15 showing a good linearity

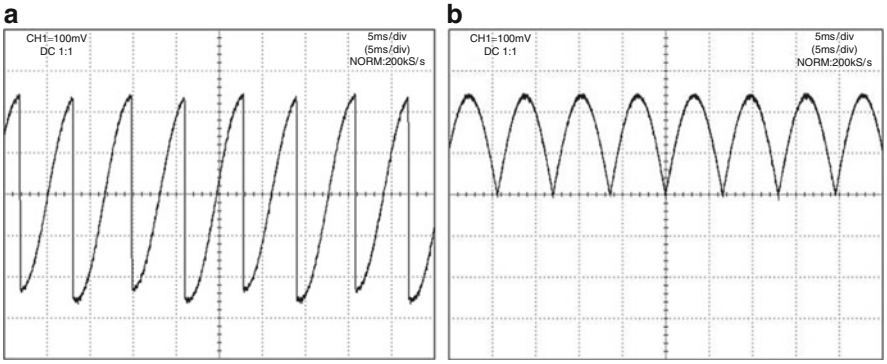

Fig. 5.13 Measurement results at the mixer output for in-quadrature (**a**) and in-phase (**b**) inputs

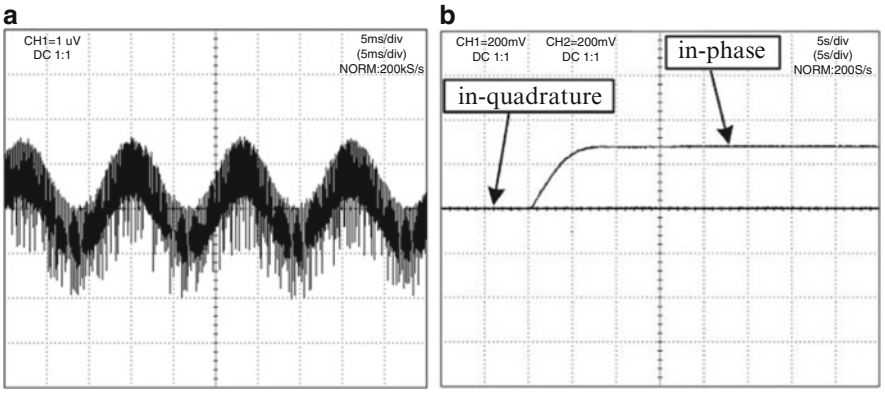

Fig. 5.14 Measured noisy input signal at the instrumentation amplifier (**a**) and the time response of the extracted DC signal at the system output with in-quadrature and in-phase input and reference signals (**b**)

between the extracted output DC voltage and the input AC noisy signal, according to the following relationship:

$$V_{OUT} = \frac{2kV_{IN}}{\pi} \tag{5.5}$$

being k the system total amplification, of about 320,000.

The fabricated system has been also tested with a suitable experimental apparatus to detect, for example, the presence of CO into a closed chamber, as shown in Fig. 5.16. In this case, for the experimental measurements, a commercial resistive gas sensor (FIGARO TGS2600, R_{SENS}) has been utilized [22], excited with a 77 Hz sinusoidal voltage signal (V_{REF} is a 77 Hz square wave signal), whose amplitude has been fixed to 40 mV, in series with a reference resistance R_{REF} valued 10 kΩ, according to the measurement block scheme depicted in Fig. 5.17.

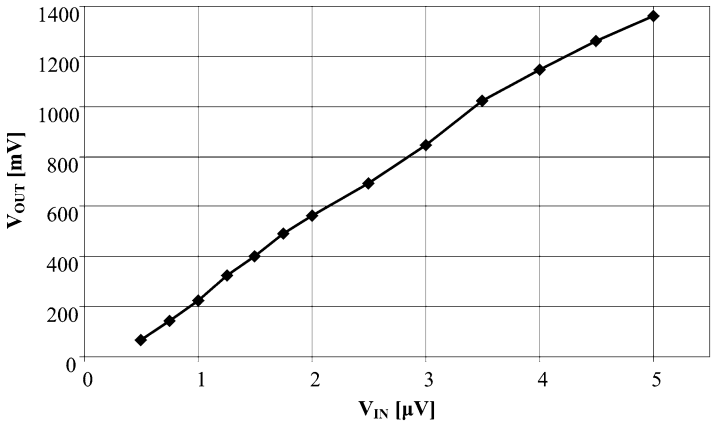

Fig. 5.15 Measured output DC voltage vs. input AC signal amplitudes (the system voltage gain A is about 110 dB)

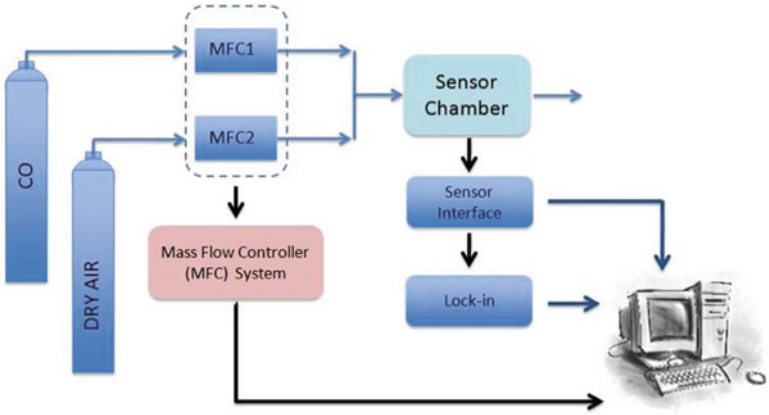

Fig. 5.16 A sketch of the experimental set-up utilized for the CO revelation

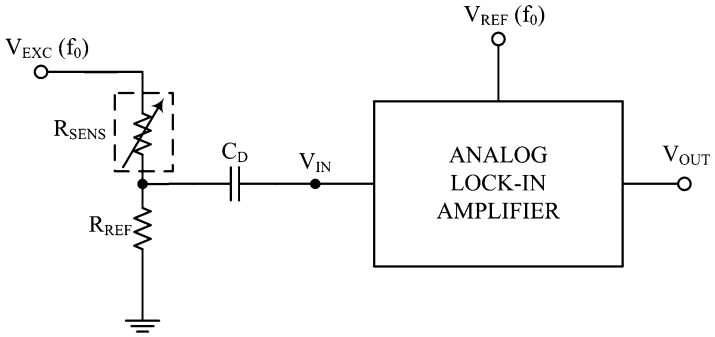

Fig. 5.17 Measurement scheme for the lock-in testing

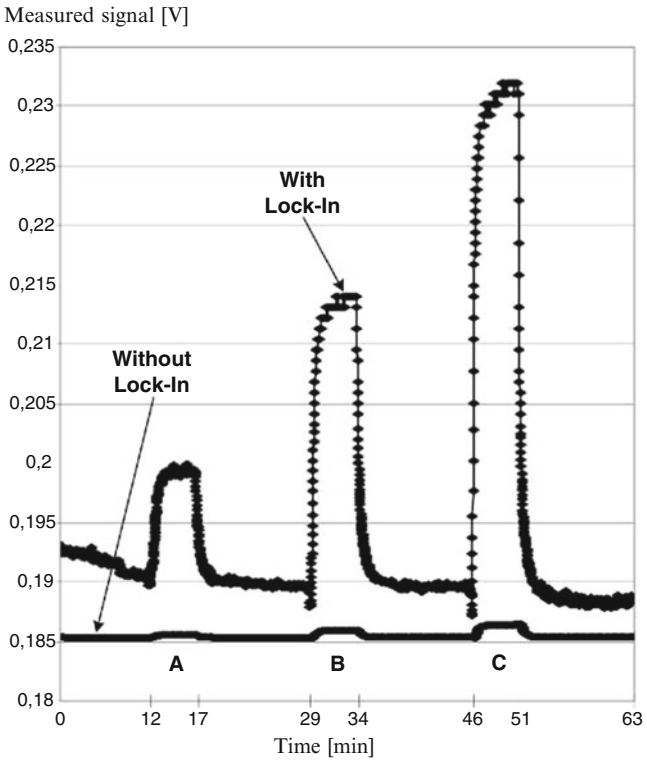

Fig. 5.18 Measured time response of the extracted DC voltage signal at the system output and voltage signal at the system input vs. time, for three different CO concentrations (A = 10 ppm, B = 20 ppm, C = 30 ppm)

In particular, in several and repetitive measurement sessions, for 5 min into a closed chamber, a mixture of dry air and *CO* at different concentrations have been fluxed, alternating it with a 12 min dry air flux. Fig. 5.18 shows the typical system time responses, considering both the input and the output voltages of the lock-in amplifier for different *CO* concentrations, as detailed in Table 5.1 (A = 10 ppm, B = 20 ppm, C = 30 ppm), where the mean values of the sensor resistance have been calculated over all the experimental measurements.

The proposed lock-in system, whose internal instrumentation amplifier operates, in this case, with a voltage gain of about 34 dB (obtained with $R_{GAIN} = 6\,\text{k}\Omega$), has improved the system sensitivity of a factor of about 40. More accurately, the system sensitivity (considered as a constant in the measured concentration range), evaluated before the lock-in amplifier application, is about 0.04 mV/ppm, while the complete analog integrated system shows an improved sensitivity of about 1.6 mV/ppm. In addition, considering the relative experimental noise levels, system resolutions before and after the lock-in amplifier are about 10 and 0.2 ppm, respectively, showing a resolution improvement, obtained through the lock-in technique, being it reduced of a factor of about 50.

Table 5.1 Experimental results achieved through the fabricated chip with related sensor resistance (R_{SENS}) estimation (see Fig. 5.18)

Measurement time [min]	CO concentration [ppm]	Mean sensor resistance < R_{SENS} > [kΩ]
0–12	–	61.1
Initial cleaning	(Dry air only)	
12–17 (A)	10	57.9
Dry air+CO mixture		
17–29	–	61.4
Cleaning	(Dry air only)	
29–34 (B)	20	53.2
Dry air+CO mixture		
34–46	–	61.5
Cleaning	(Dry air only)	
46–51 (C)	30	48.3
Dry air+CO mixture		
51–63	–	61.7
Final cleaning	(Dry air only)	

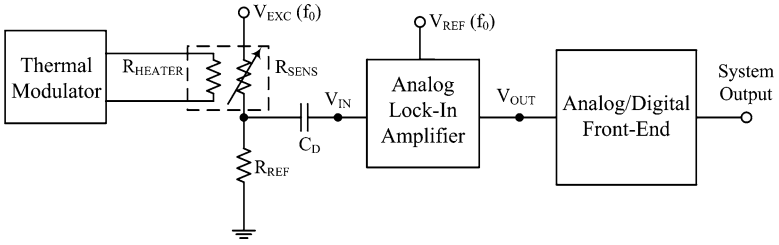

Fig. 5.19 Scheme for lock-in utilization in resistive gas sensor interface together with thermal modulation technique

Finally, the designed lock-in amplifier can also exploit the advantages of the resistive gas sensor thermal modulation (which allows to increase the sensor sensitivity), so both to further improve the whole system resolution and to detect very small quantities of gas reagent substances, very lower than 1 ppm. As an example, Fig. 5.19 shows a possible block scheme which combines the employment of these two standard techniques.

5.4 An Automatic Analog Lock-in Amplifier for Accurate Detection of Very Small Gas Quantities

In this Paragraph we want to introduce an automatic analog lock-in amplifier, together with some preliminary experimental results, which does not need the initial phase alignment and is able to recover the signal from noise also for a very low input *SNR* [23, 24].

A traditional lock-in amplifier needs the initial phase alignment of the system through the zeroing of the output signal. This means that input signals at the *PSD* block are "in quadrature". In order to reveal and measure the noisy signal at the lock-in input through the evaluation of the generated DC output signal, these two *PSD* input waveforms must be "in phase". This condition is achieved by the use of suitable control signals and switches which must be regulated and activated by manual operations. It important to highlight that an inaccurate phase alignment of the system involves measurement errors and, sometimes, also the impossibility to recover the signal.

Both in the literature and in the commercial systems, this problem has been solved through the introduction of suitable digital circuits, more complicated (*DSP* and storage elements) with respect to analog solutions, which operate a precise control of each single block employed in the system. Unfortunately, many of them, introducing a very complex architecture based on micro-processor (and/or micro-controller), for the digital signal processing, often show, consequently, large dimensions, very high costs and weight, so are not suitable for portable systems as in sensor applications [5–7, 10–12].

Starting from these considerations, a fully analog high-accuracy high-precision lock-in amplifier operating automatic phase self-alignment has been recently developed (patented system) [23, 24]. In particular, the proposed architecture allows automatically and continuously to provide the required "in phase" condition of the considered signals (automatic phase alignment of the relative phase between input and reference signals), through suitable negative feedbacks. This lock-in system allows both to perform the necessary initial phase alignment (at the power-on of the circuit) and to continuously ensure such a condition during measurement runtime (for any variation of the input noisy signal phase and amplitude during the working time), implementing a completely automatic circuit through the use of simple analog blocks. In this way, the system allows to detect, in a continuous way, the correct mean value of the input signal (buried into noise). Furthermore, no manual operations are required, avoiding errors due to input signal phase shifting, so overcoming also the problems due to temperature drifts and components aging.

Fig. 5.20 shows a possible block scheme for this automatic system. It is constituted by three main channels: "Calibration" channel, "Measure" channel and "Calibration 90°" channel. The main blocks necessary for the noisy signal recovery are the followings (standard parts of a classic lock-in): a low noise amplifier, *LNA*; a band-pass filter, *BP*; a multiplier or *PSD*, PSD_1; a low-pass filter, LP_1; a tuneable phase shifter, TPS_1 and a 90° phase shifter, TPS_2.

The operating principle of the system can be simply described as follows: the small noisy signal, introduced at the system input terminal V_{IN}, is amplified through the *LNA*, then filtered by the *BP*, so to reduce its harmonic content, and finally multiplied with the reference signal (having the same frequency of the input signal), introduced at the system input terminal V_{REF}, through the PSD_1. Finally, the filter LP_1, whose cut-off frequency has to be very small, allows to reveal the mean value of the signal generated by the PSD_1, operating an extraction of the DC component, V_{CAL}, whose value is proportional to the amplitude of the input signal and dependent

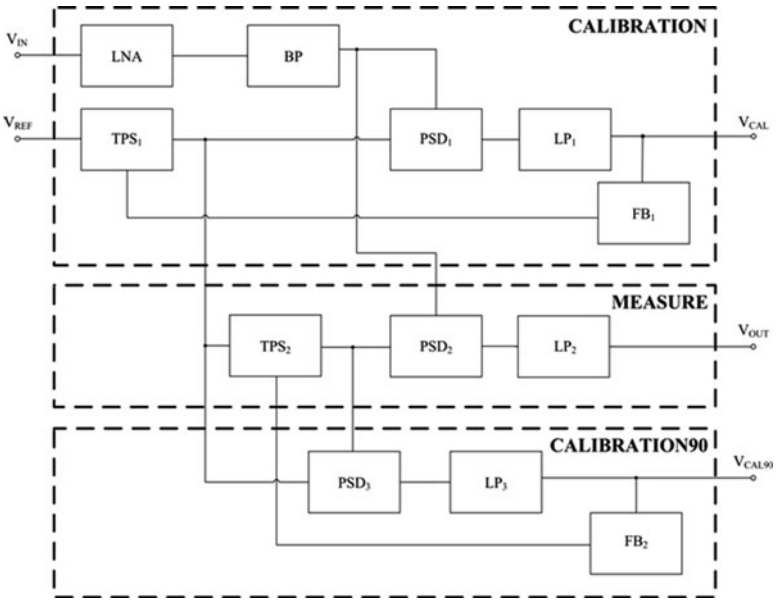

Fig. 5.20 Complete block scheme of the novel automatic analog lock-in amplifier

on its phase difference with respect to the reference signal. The precise and correct phase-alignment of the system corresponds to put the input and reference signals "in-quadrature": this is guaranteed only when the signal at LP_1 output is equal to zero. Such a condition is sustained, automatically and continuously, through suitable control blocks: the FB_1 allows to regulate opportunely the TPS_1 so that the relative phase, among input and reference signals, is always equal to 90°; at the same time, the correct measure of the DC signal V_{OUT}, whose amplitude is proportional to that of the AC input noisy signal, is achieved through the use of PSD_2 and LP_2, considering that in this case a further phase shifting of 90° between the two input signals of PSD_2 is necessary. Therefore, in order to operate and guarantee a further stable phase shifting of 90°, to be added to the relative phase among the signal coming from the PSD_1 inputs (which are "in-quadrature" by the operation of the "Calibration" channel), an additional feedback loop has been introduced. This is constituted by the blocks PSD_3, LP_3 and FB_2 which properly control the TPS_2, guaranteeing the correct relative phase delay between the input and reference signals.

This system presents two AC inputs and three DC outputs; the measured value at V_{OUT} is proportional to the input signal amplitude only when the other two calibration outputs are zero. In this sense, the final blocks of the proposed architecture are low-pass filters that reduce the noise contribution through a DC extraction.

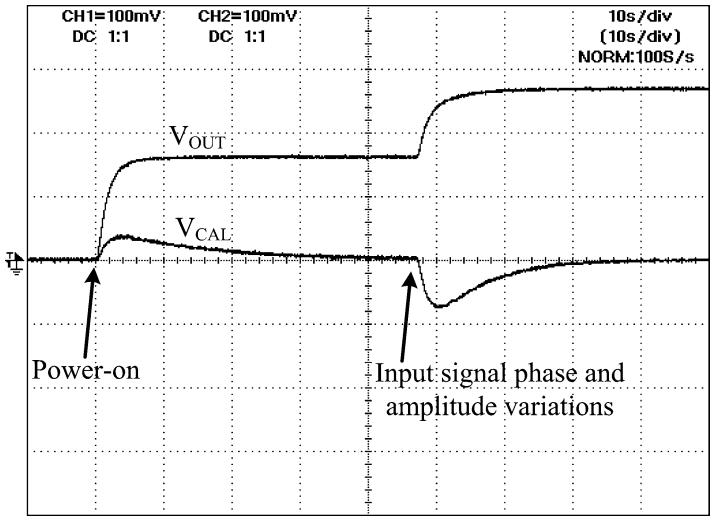

Fig. 5.21 Automatic lock-in time responses: system self-alignment at power-on followed by input signal amplitude and phase variations

The block scheme in Fig. 5.20 has been completely designed implementing the different analog blocks with suitable *VM* circuit topology, employing commercial components and precise passive elements, and then developing a discrete element prototype *PCB* (LF411 of Texas Instruments has been employed as *OA*). In particular, the *LNA* has been implemented through a well-known differential instrumentation amplifier (see Fig. 5.3), the band-pass filters have been implemented by a second-order topology (see Fig. 5.5), the low-pass filters are constituted by four *RC*-cells in cascade configuration, the *PSDs* are high-precision waveform rectifiers, while phase shifters and feedback blocks have been implemented by suitable well-known active Miller integrators. More in detail, in phase shifters, voltage controlled capacitors as electronic variable active components (i.e., AD633 of Analog Devices utilized in a suitable configuration [25]) have been utilized, achieving their tunability through the control voltage generated by relative feedback blocks.

Fig. 5.21 depicts the measured main signals V_{OUT} and V_{CAL} when an input clean sinusoidal signal has been applied, highlighting the system self-alignment at its power-on and when amplitude ($\Delta V_{IN} = 2\,\text{mV}$) and phase ($\Delta\varphi = 20°$) variations have simultaneously occurred. In particular, after a transient time due to the self-alignment operation, V_{CAL} returns at zero level, while V_{OUT} changes its DC value owing to the input signal amplitude variation.

The complete designed system has been tested by a suitable experimental apparatus (see Fig. 5.16) to detect the presence of different *CO* concentrations (10, 20 and 30 ppm), into a closed chamber, using FIGARO TGS2600 as resistive gas sensor [22]. More in detail, the commercial sensor has been excited with a 77 Hz sinusoidal voltage signal whose maximum amplitude has been fixed to 30 mV (with

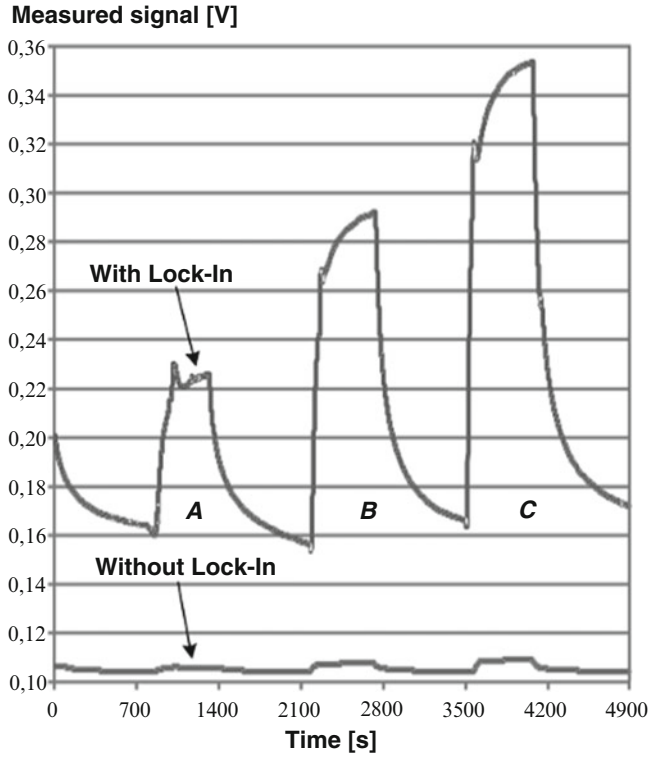

Fig. 5.22 Measured time response of the extracted DC voltage signal at the proposed lock-in output and voltage signal at the system input vs. time for different CO concentrations (CO concentrations: A = 10 ppm, B = 20 ppm, C = 30 ppm)

a DC level of 5 V), in series with a reference load resistance (see R_{REF} in Fig. 5.17) valued 10 kΩ. The sensor heater resistance has been powered with a DC voltage level equal to 5 V. In several measurement sessions, we have fluxed, for 9 min into a closed chamber, a mixture of dry air and *CO* at different concentrations, alternating it with a 14 min dry air flux. Fig. 5.22 shows the typical system time responses, considering both input and output DC lock-in amplifier signals for different *CO* concentrations, as detailed in Table 5.2 (A = 10 ppm, B = 20 ppm, C = 30 ppm), where the mean values of the sensor resistance have been reported. These voltage signals have been revealed and acquired through a *DAQ* board (NI USB-6353 by National Instruments), with a sampling rate equal to 1 s, allowing to estimate both the gas sensor resistance value and its variation, under the presence of different *CO* concentrations (see Table 5.2). Through a straightforward analysis of the experimental results and with respect to the simple resistive gas sensor interface implemented by a resistive voltage divider (as suggested by the gas sensor datasheet [22]), the sensitivity improvement given by the proposed lock-in amplifier is of a factor of about 80 (circuit input sensitivity $\approx 0.08\,\mathrm{mV/ppm}$;

Table 5.2 Experimental results achieved through the fabricated *PCB* prototype with related sensor resistance R_{SENS} estimation (see Fig. 5.22)

Measurement time [min]	CO concentration [ppm]	Mean sensor resistance $<R_{SENS}>$ [kΩ]
0–14	(Dry air only)	128
Initial cleaning		
14–23 (A)	10	91
Dry air+CO mixture		
23–37	(Dry air only)	130
Cleaning		
37–46 (B)	20	69
Dry air+CO mixture		
46–60	(Dry air only)	129
Cleaning		
60–69 (C)	30	56
Dry air+CO mixture		
69–83	(Dry air only)	129
Final cleaning		

circuit output sensitivity $\approx 6.50\,\mathrm{mV/ppm}$), while, the resolution, starting from about 5 ppm (system input resolution), has been enhanced to a calculated theoretical value of about 0.05 ppm (system output resolution), achieving an improvement factor of about 100 for a measured noise level of about 0.30 mV.

References

1. A. D'Amico, M. Faccio, G. Ferri, F. Mancini, Tecniche di rivelazione di segnale in condizioni di rapporto segnale-rumore molto minore di uno (S/N≪1), in *School of Sensors for Industrial Applications*, Portici, July 1989, pp. 467–511
2. W. Kester, *Mixed-signal and DSP Design Techniques* (Engineering Staff of Analog Devices Inc./Newnes, London, 2002). ISBN 0750676116
3. L.A. Wainshtein, *Extraction of Signals from Noise,* reprinted from (Dover Publications, Wokingham, 1970). ISBN 0486626253
4. R. Burdett, Signals in the Presence of Noise, Signal Recovery, in *Handbook of Measuring System Design* (Wiley, Wokingham, 2005). ISBN 9780470021439
5. M.L. Meade, *Lock-in Amplifiers: Principles and Applications* (Peter Peregrinus Ltd, London, 1983). ISBN 090604894X
6. Lock-in amplifiers and pre-amplifiers, Princeton Appl. Res. Corp., Datasheet, 1971
7. Lock-in amplifiers, appl. notes, Stanford Res. Sys., Datasheet, 1999
8. U. Marschner, H. Grätz, B. Jettkant, D. Ruwisch, G. Woldt, W.J. Fischer, B. Clasbrummel, Integration of a wireless lock-in measurement of hip prosthesis vibrations for loosening detection, in Proceedings of Eurosensors, Dresden, Sept 2008, pp. 789–792
9. M.O. Sonnaillon, F.J. Bonetto, A low-cost, high-performance, digital signal processor-based lock-in amplifier capable of measuring multiple frequency sweeps simultaneously. Review of Scientific Instr **76**, 024703-1-024703-7 (2005)
10. M.L. Meade, Advances in lock-in amplifiers. J. Phys. Sci. Instrum. **15**, 395–403 (1982)
11. Internet resource: http://www.signalrecovery.com. What is a Lock-in Amplifier, PerkinElmer, T.N. 1000

12. Internet resource: http://www.signalrecovery.com. PerkinElmer – The analog Lock in Amplifier, T.N. 1002
13. G. Ferri, P. De Laurentiis, C. Di Natale, A. D'Amico, A low voltage integrated CMOS lock in amplifier prototype for LAPS applications. Sensors Actuators A. **92**, 263–272 (2001)
14. G. Ferri, V. Stornelli, A. De Marcellis, M. Patrizi, A. D'Amico, C. Di Natale, E. Martinelli, A. Alimelli, R. Paolesse, An integrated analog lock-in amplifier for low-voltage low-frequency sensor interface,in *Proceedings of IWASI*, Bari, June 2007
15. A. Gnudi, L. Colalongo, G. Baccarani, Integrated lock-in amplifier for sensor applications, in *Proceedings of IEEE ESSCIRC,* Duisburg, Sept 1999, pp. 58–61
16. C. Azzolini, A. Magnanini, M. Tonelli, G. Chiorboli, C. Morandi, Integrated lock-in amplifier for contact-less interface to magnetically stimulated mechanical resonators, in *Proceedings IEEE International Conference on Design & Technology of Integrated Systems in Nanoscale Era,* 2008
17. C. Falconi, E. Martinelli, C. Di Natale, A. D'Amico, F. Maloberti, P. Malcovati, A. Baschirotto, V. Stornelli, G. Ferri, Electronic interfaces. Sensors Actuators B. **121**, 295–329 (2007)
18. M. Tavakoli, R. Sarpeshkar, An offset-canceling low-noise lock-in architecture for capacitive sensing. IEEE J. Solid-St Circ. **38**(2), 244–253 (2004)
19. A. De Marcellis, G. Ferri, V. Stornelli, E. Martinelli, C. Di Natale, A. D'Amico, Low-voltage low-power integrated CMOS analog lock-in amplifier for thermally modulated sensors,in *Proceedings of Eurosensors,* Dresden, Sept 2008
20. A. D'Amico, A. De Marcellis, C. Di Carlo, C. Di Natale, G. Ferri, E. Martinelli, R. Paolesse, V. Stornelli, Low-voltage low-power integrated analog lock-in amplifier for gas sensor applications. Sensors Actuators B. **144**(2), 400–406 (2010)
21. M. Schipani, F. Sebastiano, N. Nizza, P. Bruschi, A fully integrated very low frequency single-ended Gm-C filter based on a novel transconductor, in *Proceedings of IEEE PRIME,* Otranto, 2006, pp. 25–28
22. Internet resource: http://www.figarosensor.com. Datasheet TGS2600
23. A. De Marcellis, A. Di Giansante, C. Di Natale, G. Ferri, E. Martinelli, A. D'Amico, Analog automatic lock-in amplifier for very low gas concentration detection, in *Proceedings of Eurosensors,* vol 5, Linz, Sept 2010, pp. 200–203
24. A. De Marcellis, G. Ferri, V. Stornelli, A. D'Amico, C. Di Natale, E. Martinelli, C. Falconi, Analog system based on a lock-in amplifier for signal from noise detection showing a continuous and automatic phase alignment and frequency tuning, Patent n. RM-2008-A000194, 2008
25. G.Q. Zhong, R. Bargar, K.S. Halle, Circuits for voltage tuning the parameters of chuas circuit: experimental application for musical signal generation. J. Franklin Inst. **331 B**(6), 743–784 (1994). Elsevier